Surface concentration dependent structures of iodine on Pd(110)

Mats Göthelid, Michael Tymczenko, Winnie Chow, Sareh Ahmadi, Shun Yu, Benjamin Bruhn, Dunja Stoltz, Henrik von Schenck, Jonas Weissenrieder, and Chenghua Sun

Citation: The Journal of Chemical Physics **137**, 204703 (2012); doi: 10.1063/1.4768165
View online: http://dx.doi.org/10.1063/1.4768165
View Table of Contents: http://scitation.aip.org/content/aip/journal/jcp/137/20?ver=pdfcov
Published by the AIP Publishing

Surface concentration dependent structures of iodine on Pd(110)

Mats Göthelid,[1,a)] Michael Tymczenko,[1] Winnie Chow,[1] Sareh Ahmadi,[1] Shun Yu,[1] Benjamin Bruhn,[1] Dunja Stoltz,[1] Henrik von Schenck,[1] Jonas Weissenrieder,[1] and Chenghua Sun[2,a)]

[1]*Materialfysik, ICT Electrum 229, Kungliga Tekniska Högskolan (KTH), S-164 40 Kista, Sweden*
[2]*Australia Institute for Bioengineering and Nanotechnology, The University of Queensland, QLD 4072, Australia*

(Received 8 September 2012; accepted 3 November 2012; published online 29 November 2012)

We use photoelectron spectroscopy, low energy electron diffraction, scanning tunneling microscopy, and density functional theory to investigate coverage dependent iodine structures on Pd(110). At 0.5 ML (monolayer), a c(2 × 2) structure is formed with iodine occupying the four-fold hollow site. At increasing coverage, the iodine layer compresses into a quasi-hexagonal structure at 2/3 ML, with iodine occupying both hollow and long bridge positions. There is a substantial difference in electronic structure between these two iodine sites, with a higher electron density on the bridge bonded iodine. In addition, numerous positively charged iodine near vacancies are found along the domain walls. These different electronic structures will have an impact on the chemical properties of these iodine atoms within the layer. © *2012 American Institute of Physics*. [http://dx.doi.org/10.1063/1.4768165]

INTRODUCTION

Palladium is one important transition metal used in both homogeneous and heterogeneous catalysis. Organo-halides are often used to form reactive carbon fragments,[1] which leave a halogen coordinated to the catalyst metal. Depending on the coordination site and charge transfer between surface and adsorbate, the surface halide may act as a catalyst poison[2] or as a key factor in controlling chemical selectivity.[3] This effect on selectivity is related to the strength of the palladium-halide interaction and the surface bond geometry. Moreover, halogens are used to etch metals[4] and semiconductors[5] and a fundamental understanding of halogen surface properties is crucial. Iodine/iodide is often used as redox couple in dye sensitized solar cells (the Grätzel cell).[6] It was recently reported that the concentration of iodine in the electrolyte affects the output from the solar cell.[6] The results were discussed in terms of ionic mobility of tri-iodide, chemical availability, recombination losses, and light absorption interference with the dye.[6] However, the iodine chemistry on the metal electrode was not discussed in detail. In order to gain a broader understanding of iodine chemistry, structures, and charge transfer processes, we have studied iodine sub-monolayer structures on various metals (Pd, Pt, Au, Cu, Zn) using scanning tunneling microscopy (STM), photoelectron spectroscopy (PES), and density functional theory (DFT). Here, we report an investigation of iodine-induced structures on Pd(110).

Iodine was previously studied on Pd(110) where two ordered structures were found: c(2 × 2) at 0.5 ML (monolayer) iodine coverage and a flat quasi-hexagonal (q-hex) structure at higher coverage.[7] A similar scenario was observed for iodine on Cu(110), where the quasi hexagonal phase was observed at ∼0.67 ML co-existing with an ordered CuI phase.[8] The quasi hexagonal phase was explained by a compression of the iodine layer along the ⟨−110⟩ direction.[8] The idea of the formation of a compressed quasi hexagonal phase was earlier proposed by Bardi and Rovida from their work on Ag(110)-I,[9] and by Erley for Cl on Pd(110).[10] One possible iodine adsorption site in the c(2 × 2) structure is the four fold hollow position as proposed in Refs. 7–9. On Ag(110), it was instead proposed from density functional theory (DFT) that short bridge adsorption is preferred over top, hollow, and long bridge, in order of decreasing preference.[11] What are the electronic and chemical properties of iodine sitting in different sites? We find that iodine occupies hollow sites up to 0.5 ML coverage and then gradually also fills long bridge sites. The electronic properties differ significantly in these two sites, and consequently their chemical properties.

EXPERIMENTAL METHODS

The photoemission experiments were performed at beam line I511, at MAX-lab, in Lund, Sweden. The beam line is undulator based using a modified SX-700 monochromator.[12] The photoemission spectra were recorded in normal emission with a Scienta SES200 electron spectrometer.[13] Pd $3d_{5/2}$ spectra were acquired at 405 eV and 453 eV photon energies. The I4d core level spectrum was recorded at 134 eV. The total experimental resolution was ca. 40 meV for the I4d and 120 meV for the Pd3d spectra. STM experiments were done in a RHK 3500 UHV STM using cut PtIr tips in constant current mode.

The sample was prepared in preparation chambers connected to the photoemission and STM chambers via gate valves. These chambers are equipped with low energy electron diffraction (LEED) optics, Ar-ion sputter gun, and sample heating. The samples were mounted on Ta-sample holders. Sample temperatures were measured with chromel-alumel thermocouples, spot-welded on the side of the sample or by a

a)Authors to whom correspondence should be addressed. Electronic addresses: gothelid@kth.se and c.sun1@uq.edu.au.

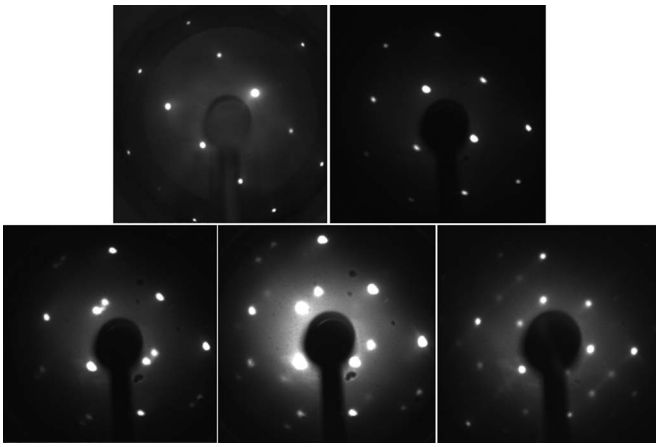

FIG. 1. LEED patterns from the (1 × 1) (upper left) at 95 eV and c(2 × 2) (upper right) at 78 eV. Lower row are photographs from the quasi-hexagonal structure at 72 eV and 66 eV, respectively, and finally a (3 × 2) pattern in the low right hand picture. The (0,0) spot is the spot just low-left of the electron gun.

pyrometer. The Pd(110) sample was prepared by argon sputtering and oxygen treatment at high temperatures (P_{O2} = 2–5 × 10^{-7} Torr, 530 °C), followed by flashing to 830 °C in order to obtain a clean and well-ordered surface. The cleanliness of the surface was checked by PES and LEED.

Iodine was deposited onto the surface at room temperature from an electrochemical cell, consisting of an AgI pellet heated to ∼100 °C.[14] Exposures were measured in μA.minute, i.e., the ionic current going through the cell (10 μA in this case) times the duration of the evaporation. On Pd(110) deposition of 200 μA.min, I_2 at room temperature resulted in the q-hex structure, which transformed to c(2 × 2) after annealing at 350 °C. The iodine coverage on the c(2 × 2) surface was estimated to be 0.52 ± 0.03 ML from the I4d intensity compared to the Pd(111)-I ($\sqrt{3}$x$\sqrt{3}$)R30° surface with 0.33 ML coverage.[15] The coverage in the quasi hexagonal structure cannot be accurately determined using this method due to photoelectron diffraction effects that renders different results at different photon energies. However, based on the previous study on Cu(110)-I[8] and our STM, we believe that the q-hex coverage is close to 2/3 ML.

COMPUTATIONAL METHODS

Spin-polarized density functional theory (DFT) calculations have been performed within the generalized-gradient approximation (GGA),[16] with the plane-wave basis (cutoff energy: 380 eV) and the exchange-correlation functional of Perdew-Burke-Ernzerhof (PBE),[17,18] as implemented in the Vienna *ab initio* simulation package (VASP).[19,20] Total energy and maximum force are converged to 10^{-4} eV and 0.05 eV/Å, respectively, and the k-space is sampled by a Monkhorst-Pack mesh with the distance between any neighboring k-points less than 0.025/Å. Atomic populations are analyzed based on the Bader approach,[21] and Mulliken analysis[22] has also been carried out using another plane-wave DFT code–CASTEP[23] and similar results are obtained. Pd(110) is modeled by slab models (11 Pd layers, with a thickness of 14.30 Å) for two supercells, (2 × 2) and (3 × 2), based on which five coverages θ for iodine adsorption have been investigated with θ = 1/6, 1/4, 1/2, 2/3, and 1 monolayer (ML). The use of a (3 × 2) cell is motivated by the fact that this is one possible structure following compression in the ⟨−110⟩ direction. It was also occasionally observed in LEED.

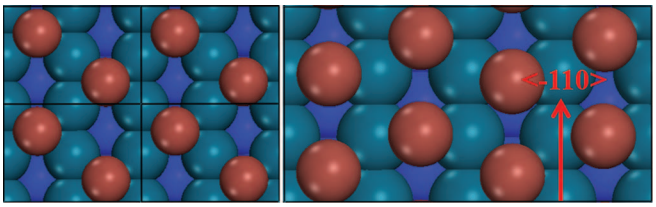

FIG. 2. Optimized structure models at different iodine coverage; green balls represent Pd and red balls represent iodine. The left hand figure is the c(2 × 2) structure at 0.5 ML coverage and the right hand figure is a 3 × 2 structure at 0.67 ML iodine coverage. Iodine atoms are shown as red spheres, and palladium atoms at the top and second layers are shown as cyan and blue spheres, respectively.

RESULTS AND DISCUSSION

Representative LEED pictures are shown in Figure 1 below. The original (1 × 1) pattern is shown in the top left image while a picture from the c(2 × 2) structure is displayed in the top right hand picture. The two lower images from the q-hex structure were recorded at different electron energies. At increasing energy, the spots in the centre of the zone split and move apart. A similar behavior was observed for Cu(110)-I[8] and was interpreted as a compression of the iodine layer in the ⟨−110⟩ direction. This compression resulted in a non-uniform domain wall structure with a quasi hexagonal atomic structure. Occasionally, we also observed a (3 × 2) LEED pattern. This pattern was only observed irregularly, but it proves that the (3 × 2) structure indeed exists.

Our theoretical calculations were first done in order to find the energetically most stable structures at different iodine coverage. At low coverage, iodine prefers to stay at the hollow site, and with increasing coverage, iodine starts occupying bridge sites. In Figure 2 optimized geometries for θ = 1/2 ML and θ = 2/3 ML are present, corresponding to c(2 × 2) and (3 × 2) patterns. Adsorption energies and atomic population (AP) for iodine adsorbed at different sites are given in shown in Table I. As indicated by the adsorption energies, hollow sites offer stronger adsorption capacity because each iodine at hollow site bonds with five Pd atoms.

In Figure 3, we present atomically resolved STM images from Pd(110)-I c(2 × 2), recorded at 4 mV tunnel bias and 0.2 nA tunnel current. The atomically resolved structure is in

TABLE I. Calculated adsorption energies and atomic populations (Bader analysis) for iodine in hollow and bridge positions on the c(2 × 2) and (3 × 2) structures.

	E_{ads} hollow (eV)	E_{ads} bridge (eV)	AP_I hollow (e)	AP_I bridge (e)
c(2 × 2)	3.33		7.01	
(3 × 2)	3.26	2.96	7.01	7.10

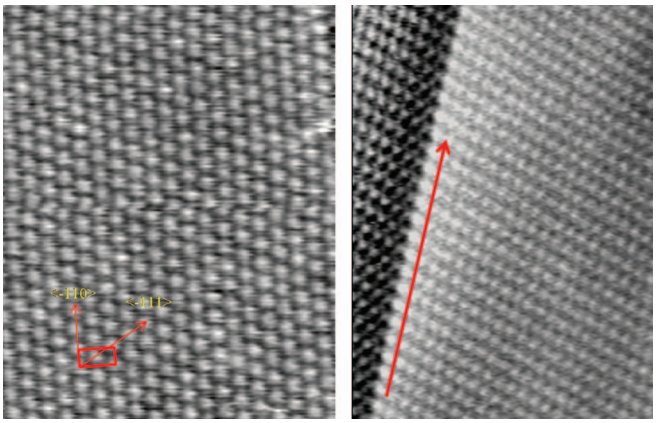

FIG. 3. Atomically resolved STM images from the Pd(110)-I c(2 × 2) phase together with atomic structure models. Atomic distances are 5.5 Å in ⟨−110⟩ and 4.8 Å in ⟨−111⟩.The long red arrow points along ⟨−110⟩.

splendid agreement with the atomic model in Figure 2(a). In Figure 3(a), a (2 × 2) unit cell has been added together with crystallographic directions. The atomic distances are 5.50 Å in the ⟨−110⟩ direction and 4.76 Å along the ⟨−111⟩ direction, which is the shortest distance between iodine. The height corrugation is 0.2 Å. Figure 3(b) contains two terraces separated by a step running along the ⟨−111⟩ direction. The atomic corrugation in this image is ∼ 0.1 Å.

Figure 4 was recorded at an intermediate coverage with the c(2 × 2) phase in the lower left and upper right corners coexisting with the compressed phase in the central part of the image. While the c(2 × 2) structure nicely follows the terrace edges, the compressed phase comprise domain walls rotated away from the terrace edge direction. The angle between the two arrows, **a** and **b**, in the image is ∼30°. From the LEED pattern and the discussion in Ref. 8, the compression should be in the ⟨−110⟩ direction. The angle between ⟨−110⟩ and ⟨−111⟩ is 35°, in fair agreement with the measured angle in the image. Furthermore, the atomic lines perpendicular to the step edges are still straight, in agreement with a unidirectional compression. A close look at the wave structure, along arrow **b**, gives that the lines are not perfectly straight, but has local variations. This is similar to observations on Cu(110)-I.[8] The corrugation is believed to originate in a compression of the iodine layer, which shifts iodine away from the hollow position into long bridge.[8] The long bridge and hollow (and transitions between them) are the only available sites if the c(2 × 2) structure is compressed along ⟨−110⟩. On Cu(110), c(8 × 2) structures were observed, including domain walls with locally higher iodine coverage. In order to relieve strain on the iodine, there is a shift of the domain walls out of phase along the short end of the unit cell. In our case, we do not observe a c(8 × 2) ordering, but we do observe a large number of vacancies in the structure, which also relieve the local pressure.

Figure 5 was recorded from the fully developed q-hex phase, where the atomic structure is resolved between the domain walls. The structure resembles the c(2 × 2) structure, but the atomic distances are compressed and it also contains defects around which the distances are different. Atoms near defects appear higher, due to an increased density of electronic states near the Fermi level. Interestingly, the domain

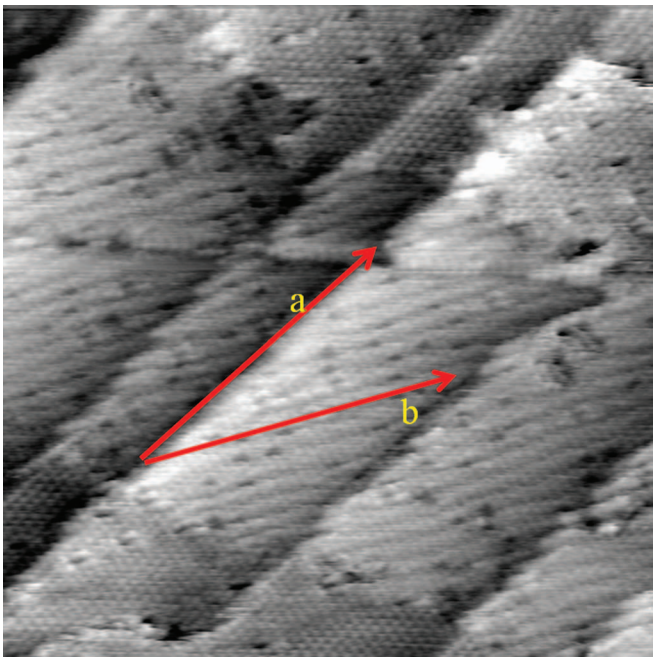

FIG. 4. STM image of mixed the c(2 × 2) and q-hex phases.

walls appear brighter on defects rich areas. Furthermore, the atomic distances are different in areas with different amounts of defects. These observations suggest that the iodine overlayer is rather flexible, both in terms of atomic geometry and electronic structure. Our model in Fig. 2(b) is made of equal amounts of hollow and long bridge adsorbed iodine. The model is not exactly representing the structure observed in the STM image, but by compressing the c(2 × 2) structure along ⟨−110⟩, the only possible atomic positions for iodine are hollow, long bridge and transitions between them. We believe that a model with hollow and long bridge will represent this system fairly well.

CORE LEVEL SPECTROSCOPY

Electronic structure variations are reflected in site dependent core level binding energies. $Pd3d_{5/2}$ spectra from Pd(110) (1 × 1) and Pd(110)-I c(2 × 2) are presented in Figure 6; the two upper spectra from (1 × 1) and the two lower spectra from c(2 × 2). Photon energies are indicated in connection to respective spectra. We present two different line profile

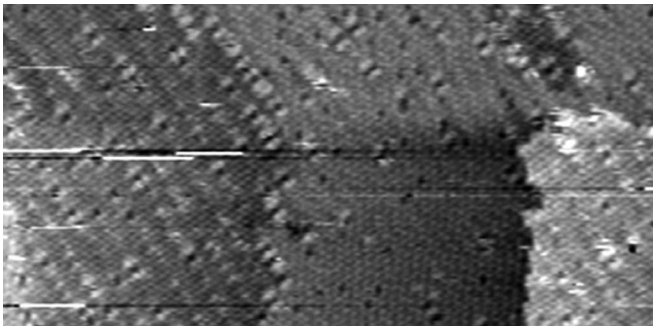

FIG. 5. STM image from the q-hex phase, recorded at 4 mV negative tip bias.

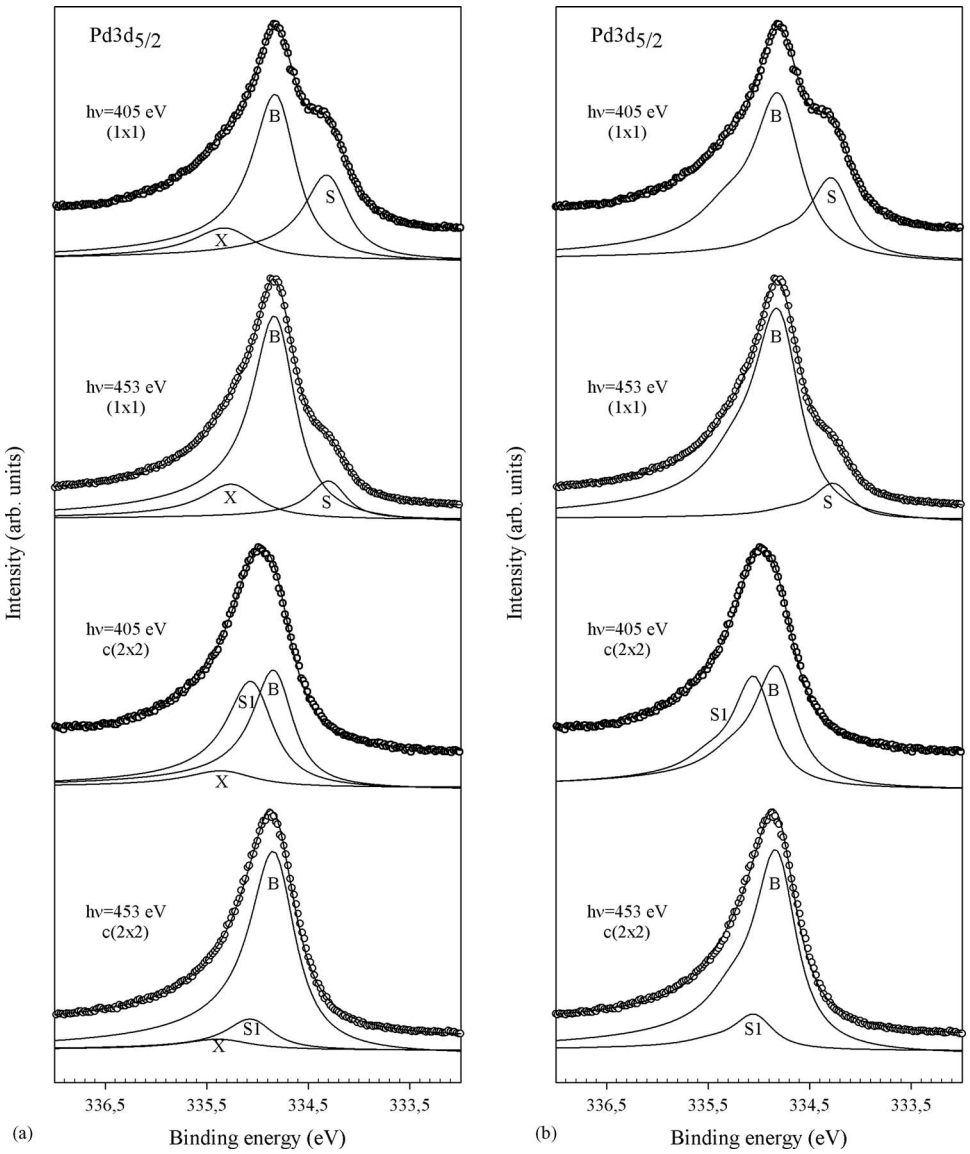

FIG. 6. $Pd3d_{5/2}$ core level spectra recorded at 405 eV and 453 eV photon energies from the (1 × 1) and c(2 × 2)-I structures. Numerical fitting of the spectra were done using two different methods; (a) with Doniach-Sunjic lines and in (b) with a built-in loss feature.

analyses giving the same result: a surface core level shift 0.52 ± 0.02 eV to lower binding energy on the clean surface and a 0.22 ± 0.02 eV shift to higher binding energy on the c(2 × 2)-I surface.

Curve fitting using Doniach-Sunjic line profiles[24] has failed to properly describe the Pd3d core level spectrum, in particular on the high binding energy side, due to the rapidly varying density of states around the Fermi level.[25–27] For this reason, very few fitted high resolution spectra from clean palladium surfaces are found in the literature. Close inspection often reveals a small "hump" in spectra at very high resolution.[26–29] This apparent problem disappears upon adsorption, since many adsorbates induce core level shifts on that side of the spectrum, and therefore fitted spectra are much more often seen after adsorption.

In the left-hand figure, we present results of a fit where, in addition to the bulk and surface contributions, an extra component X has been introduced. With this component added, stable and reproducible fits of all four spectra are obtained using exactly the same line profile for all components: Gaussian width 0.15 eV, Lorentzian width 0.41 eV, and asymmetry parameter 0.13. The X component is shifted 0.51 eV from the bulk peak position and the relative intensity is 15% independent of photon energy. On the clean unreconstructed surface, the surface component is identified from the reduced intensity on the low binding energy side in the 453 eV spectrum in which the electron mean free path can be expected to be longer than at 405 eV photon energy.[26] The surface to bulk intensity is 0.51 in the top-most spectrum and 0.16 in the 453 eV spectrum. Having a surface shift to lower binding energy is in good agreement with previous reports on this and other low index Pd surfaces.[26–31]

After the formation of the c(2 × 2) structure, new spectra were recorded. They are presented in the two lower panels of Figure 6. We again use three components to reproduce the experimental spectra: bulk (B), surface (S1), and extra (X).

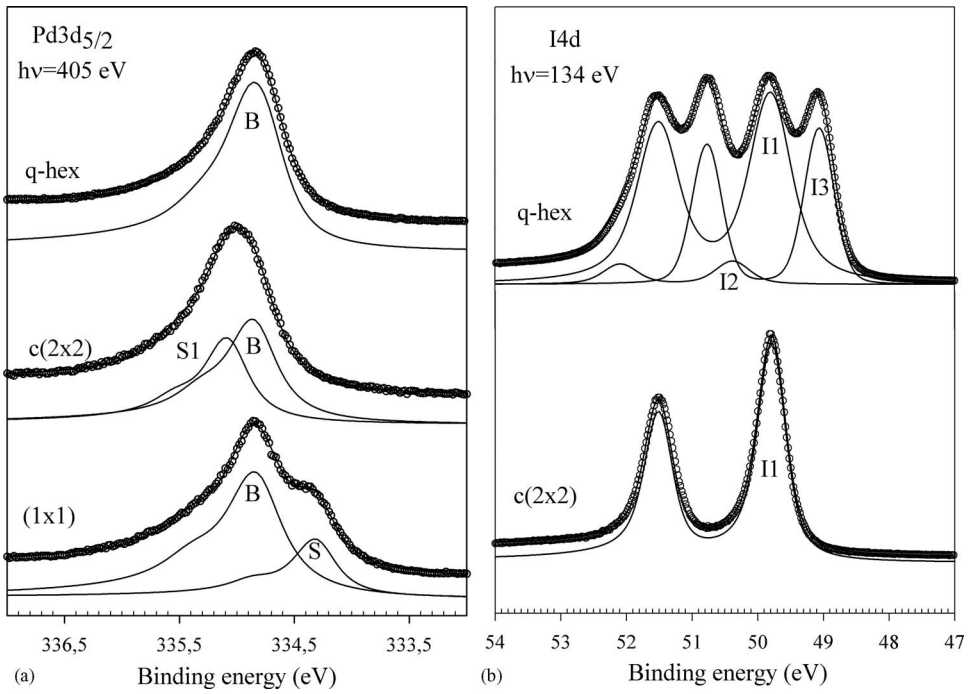

FIG. 7. (a) $Pd3d_{5/2}$ and (b) I4d core level spectra recorded from the (1 × 1), c(2 × 2)-I, and quasi hexagonal (q-hex) structures.

The need for the surface peak is seen on the width and shape around the peak maximum of the spectrum. Again, the surface contribution is identified from the variation in relative intensity between the two photon energies. Here, the surface to bulk ratio is 0.94 at 405 eV photon energy, while it is 0.16 at 453 eV. The iodine induced surface core level shift is 0.22 ± 0.02 eV to higher binding energy, while the X peak remains on the same 0.52 eV from the bulk peak. It has a lower intensity in this structure.

An alternative method to extract surface core level shifts in these spectra is based on the idea of Nyholm *et al.*[26] who identified Pd3d surface and bulk contributions from Pd(100) by using a subtraction procedure utilizing the adsorption of hydrogen to take out the surface core level shift on that surface. We applied a similar analysis of the Pd(111) (1 × 1) and Pd(111)-I ($\sqrt{3}$x$\sqrt{3}$) surfaces.[15] The resulting surface core level shift and relative intensities compared very well with other literature (see Ref. 15). Here, we apply a similar method to the Pd(110) surface with and without iodine in a c(2 × 2) structure. The model function is a main line and a "built-in" loss feature in each component, the relative intensity, and energy separation from the main peak is adjusted in the fit. The separation was optimized to be the same 0.47 eV in all four spectra and the relative intensity is 11% of the host peak. The results are presented in Figure 6(b). The surface core level shift on the clean surface is 0.53 ± 0.02 eV. At 405 eV photon energy, the surface to bulk intensity ratio is 0.49 while it is 0.17 at 453 eV. Analyzing Pd3d from the c(2 × 2)-I structure reveals a 0.22 eV surface core level shift to higher binding energy compared to the bulk. The surface-to-bulk ratio is 0.91 and 0.16, respectively. Thus, the energy shifts and relative intensities are practically the same in the two methods of analysis, except for the X-component. Each component in a fit should represent separate chemical or electronic species on the surface; i.e., atoms in different sites or bonding configurations. We believe that the X-component does not represent a group of atoms on the surface, but reflects excitations across the Fermi level made by the outgoing photoelectron, and the fit using built in loss is a better representation.

Pd3d spectra recorded from three surfaces; (1 × 1), c(2 × 2), and quasi hexagonal, are presented in Figure 7. The difference between (1 × 1) and c(2 × 2) is rather large, as already seen in Figure 6. The surface shifted component on the unreconstructed surface (S) is replaced for a new component (S1) on the c(2 × 2). The shift to higher binding energy in c(2 × 2) indicates a slightly oxidative effect of iodine on Pd. Unexpectedly, the S/B ratio is larger on c(2 × 2) than on (1 × 1), both structures hold 1 ML of chemically shifted surface Pd atoms. However, at 453 eV (Figure 6), the ratios are closer. This indicates significant photoelectron diffraction effects.

Spectral changes between c(2 × 2) and quasi-hexagonal are not directly obvious. However, the surface shifted component in the c(2 × 2) phase has disappeared as seen in the curve fit. We kept the line profile the same in all spectra except for the position and the width. The single component in the q-hex phase is slightly broader, but in all other respects it has the same line profile. The binding energy also coincides with the bulk binding energy on the (1 × 1) and c(2 × 2) surfaces. Thus, we conclude that Pd3d from q-hex is nicely fit with one single component. This finding may seem surprising at first since there still is one monolayer of Pd atoms beneath the iodine layer. One possible explanation is that the compact iodine layer adapts several slightly different adsorption geometries that render small but slightly different surface shifts, leading to broadening rather than clear components.

The I4d spectra recorded from the Pd(110)-I c(2 × 2) and quasi hexagonal surfaces at hν = 134 eV are presented

in Figure 7. One single component at 51.51 eV is sufficient to reproduce the experimental c(2 × 2) spectra, which supports a single chemisorption site on the surface. The spectrum from the quasi hexagonal phase is spectacularly different incorporating three components. We take I1 to represent iodine in hollow sites, the same as in the c(2 × 2) phase. The remaining two components are, based on the relative intensities, tentatively assigned to; iodine near defects (I2) and iodine in bridge sites (I3). The chemical shift between I1 and I3 is 0.89 eV and indicates that there is a rather serious electronic difference between the two sites. We calculated the chemical shift from the (3 × 2) model giving a 0.80 eV energy separation, in good agreement with our experiment. Thus, although the model does not perfectly represent the actual atomic structure on the surface, it captures the main features of our core level spectra and we believe that hollow and long-bridge adsorption sites are most common on this surface.

Typically, a shift to lower binding energy is interpreted as being due to a more electron rich environment, while a shift to higher binding energy is typical for oxidation, i.e., a reduced electron density on those atoms. Such interpretation is perhaps over simplified; one has to take final state effects into account. What happens when the photoelectron has left? The positive core hole attracts the surrounding electron cloud, and the more available those electrons are in terms of density and mobility the better screened is the hole. A poorer screening leads to a higher apparent binding energy and better screening leads to lower binding energy. Our observation thus suggests that bridge bonded atoms have access to more electrons, either in the initial and/or the final state, which agrees well with the calculated atomic populations shown in Table I.

This discussion would also suggest that the iodine responsible for the I2 component has a reduced electron density. STM indicated a fair amount of defects, atomic vacancies in the iodine layer. Neighboring atoms appear higher in the empty state STM image. A majority of those defects are located on the domain walls, which can be associated with the bridge site iodine. Thus, from the combined core level and STM results, we suggest that vacancies appear more frequently on the bridge site, and neighboring atoms are charge positively. The relative I1/I3 intensity indicates a higher occupation of hollow than bridge sites. This is in line with the removal of some bridge bonded iodine and also a core level shift on neighboring atoms (to I2), both reducing the I3 intensity.

The different geometrical and electron densities on atoms within the iodine monolayer will translate to different chemical properties and charge transfer abilities. Our findings demonstrate the importance of both surface structure and surface concentration of iodine on the properties and performance of a monolayer. It also shows that I4d core level spectroscopy can be a useful tool to identify chemical differences within an iodine layer.

CONCLUSIONS

We have used core level PES, LEED, STM, and DFT to investigate iodine induced c(2 × 2) and quasi hexagonal structures on Pd(110). Two adsorption sites dominate; hollow and long-bridge, with a higher electron density on bridge bonded iodine, leading to a large chemical shift I4d spectra as observed both experimentally and theoretically. Moreover, the surface layer hosts a number of vacancies, preferentially at the bridge-bonded sites, that are charged positively. These variations within the iodine layer underline the importance of surface structure and surface density on chemical and electronic properties.

ACKNOWLEDGMENTS

This work was supported by the Swedish Research Council (VR), the Swedish Energy Agency (STEM), and the Göran Gustafsson Foundation. H.v.S. would like to thank the Ernst Johnson Foundation for a grant. C.H.S. thanks the generous grants of the CPU time from Australia NCI facilities and HPC cluster in The University of Queensland. We would also like to thank the MAX-lab staff for help at the beam-line.

[1] J. P. Collman, L. S. Hegedus, J. R. Norton, and R. G. Finke, *Principles and Applications of Organo-transition Metal Chemistry*, 2nd ed. (University Science Books, Mill Valley, CA, 1987).
[2] M. P. Kiskinova, *Poisoning and Promotion in Catalysis based on Surface Science Concepts and Experiments*, Studies in Surface Science and Catalysis (Elsevier, 1992).
[3] W. Cabri and I. Candiani, Acc. Chem. Res. **28**, 2 (1995).
[4] E. Dona, M. Cordin, C. Diesl, E. Bertel, C. Franchini, R. Zucca, and J. Redinger, J. Am. Chem. Soc. **131**, 2827 (2009).
[5] W. Simpson and J. A. Yarmoff, Annu. Rev. Phys. Chem. **47**, 527 (1996).
[6] Ze Yu, M. Gorlov, J. Nissfolk, G. Boschloo, and L. Kloo, J. Phys. Chem. **114**, 10612 (2010).
[7] W. F. Themesgen, J. B. Abreu, R. J. Barriga, E. A. Lafferty, M. P. Soriaga, K. Sashikata, and K. Itaya, Surf. Sci. **385**, 336 (1997).
[8] B. V. Andryushechkin, K. N. Eltsov, and V. M. Shevlyuga, Surf. Sci. **584**, 278 (2005).
[9] U. Bardi and G. Rovida, Surf. Sci. **128**, 145 (1983).
[10] W. Erley, Surf. Sci. **114**, 47 (1982).
[11] H. R. Tang, W. N. Wang, Z. H. Li, W. L. Dai, K. N. Fan, and J. F. Deng, Surf. Sci. **450**, 133 (2000).
[12] R. Denecke, P. Väterlein, M. Bässler, N. Wassdahl, S. Butorin, S. A. Nilsson, J. E. Rubensson, J. Nordgren, N. Mårtensson, and R. Nyholm, J. Electron Spectrosc. Relat. Phenom. **101–103**, 971 (1999).
[13] N. Mårtensson, P. Baltzer, P. Brühwiler, J-O. Forsell, A. Nilsson, A. Stenborg, and B. Wannberg, J. Electron Spectrosc. Relat. Phenom. **70**, 117 (1994).
[14] N. D. Spencer, P. J. Goddard, P. W. Davies, M. Kitson, and R. M. Lambert, J. Vac. Sci. Technol. A **1**, 1554 (1983).
[15] M. Göthelid, H. von Schenck, J. Weissenrieder, B. Åkermark, A. Tkatchenko, and M. Galvan, Surf. Sci. **600**, 3093 (2006).
[16] W. Kohn and L. J. Sham, Phys. Rev. **140**, A1133–A1138 (1965).
[17] J. P. Perdew, K. Burke, and M. Ernzerhof, Phys. Rev. Lett. **77**, 3865 (1996).
[18] G. Kresse and D. Joubert, Phys. Rev. B **59**, 1758 (1999).
[19] G. Kresse and J. Furthmüller, Phys. Rev. B **54**, 11169 (1996).
[20] G. Kresse and J. Furthmüller, Comput. Mater. Sci. **6**, 15 (1996).
[21] R. F. W. Bader, S. G. Anderson, and A. J. Duke, J. Am. Chem. Soc. **101**, 1389 (1979).
[22] R. S. Mulliken, J. Chem. Phys. **36**, 3428 (1962).
[23] S. J. Clark, M. D. Segall, C. J. Pickard, P. J. Hasnip, M. J. Probert, K. Refson, and M. C. Payne, Z. Kristallogr **220**, 567 (2005).
[24] See, for example, O. Björneholm, A. Nilsson, H. Tillborg, P. Bennich, A. Sandell, B. Hernnäs, C. Puglia, and N. Mårtensson, Surf. Sci. **315**, L983 (1994) and references therein; S. Doniach and M. Sunjic, J. Phys. **C3**, 285 (1970).
[25] G. K. Wertheim and P. H. Citrin, *Photoemission in Solids I*, in Topics in Applied Physics, edited by M. Cardona and L. Ley (Springer, 1978).

[26]R. Nyholm, M. Qvarford, J. N. Andersen, S. L. Sorensen, and C. Wigren, J. Phys. Condens. Matter **4**, 277 (1992).
[27]S. Surnev, M. Sock, M. G. Ramsey, F. P. Netzer, M. Wiklund, M. Borg, and J. N. Andersen, Surf. Sci. **470**, 171 (2000).
[28]J. N. Andersen, M. Qvarford, R. Nyholm, S. L. Sorensen, and C. Wigren, Phys. Rev. Lett. **67**, 2822 (1991).
[29]A. J. Jaworowski, R. Ásmundsson, P. Uvdal, and A. Sandell, Surf. Sci. **501**, 74 (2002).
[30]M. G. Ramsey, F. P. Leisenberger, F. P. Netzer, A. J. Roberts, and R. Raval, Surf. Sci. **385**, 207 (1997).
[31]J. N. Andersen, D. Hennig, E. Lundgren, M. Methfessel, R. Nyholm, and M. Scheffler, Phys. Rev. B **50**, 17525 (1994).